INSIGHTS INTO FAYALITE FORMATION THROUGH SECONDARY PROCESSES: AN EXPERIMENTAL AND A MICROSTRUCTURAL INVESTIGATION. E. Dobrică[1], K. K. Ohtaki[1], J. A. Nuth[2], and A. J. Brearley[3], [1]Hawai'i Institute of Geophysics and Planetology, School of Ocean, Earth Science, and Technology, the University of Hawai'i at Mānoa, Honolulu, Hawaii 96822 USA, dobrica@hawaii.edu. [2]Solar System Exploration Division, Code 690, NASA Goddard Space Flight Center, Greenbelt MD 20771 USA. [3]Department of Earth and Planetary Sciences, MSC03-2040, 1 University of New Mexico, Albuquerque, NM 87131-0001, USA.

Introduction: As seen with the samples from comet 81P/Wild 2 returned by the Stardust mission, it is extremely valuable to compare meteoritic and synthetic experimental samples with returned samples from a known body. Laboratory experiments designed to constrain the conditions that were active during the earliest stages of parent body evolution could help us understand the secondary processes that modify the pristine components of chondrites. Therefore, in this study, we use an experimental approach to gain additional insights into the fluid composition and the growth of FeO-rich olivine, which is one the most abundant secondary phases in the matrices of weakly metamorphosed petrologic type 3 chondrites [1-3]. These characteristics are essential to give context to future returned samples such as those from the Hayabusa2 and OSIRIS-REx missions. In this study, we investigate the mineralogy, texture, chemical composition, and crystallography of synthetic FeO-rich olivines formed during laboratory experiments.

Sample and methods: We performed one hydrothermal alteration experiment to synthesize FeO-rich olivines. The reactants (FeO-rich amorphous silicates, iron metal powder, and water) were loaded in a gold capsule. The experiment was carried out at a temperature of 220°C for a period of 6 days. Details of the synthesis method for FeO-rich olivine (Fa_{100}) are outlined in [1-2]. The reactants and products of the hydrothermal experiment were first characterized by scanning electron microscopy (SEM) using backscattered electron imaging on a Helios 660 dual-beam focused ion beam SEM (FIB-SEM) instrument at the Advanced Electron Microscopy Center (AEMC) at UH Mānoa. Three electron transparent sections were prepared by the *in situ* FIB technique. Each FIB section was studied using a variety of TEM techniques, including scanning transmission electron microscopy (STEM) imaging, nanodiffraction, and energy-dispersive X-ray spectroscopy (EDS). All imaging and analysis were carried out at 300 kV using the Titan G2 analytical (S)TEM. Crystalline phases were identified by electron nanodiffraction and EDS. Nanodiffraction was carried out with an accelerating voltage of 300 kV, a camera length of 295 mm, and a convergence angle of α = 0.1–0.3 mrad.

Results: Elongated, radiating intergrowths of multiple fayalite crystals were identified in the products of the hydrothermal experiment (Fig. 1-2). The majority of the elongated crystals are elongated parallel to the c^* direction (Fig. 2b). Most of these synthetic fayalite crystals have highly irregular surfaces. These features are characterized by pillar-like textures with sizes up to 300 nm in height (Fig. 2d).

Additionally, the synthetic fayalite crystals contain abundant, nanometer-size pores (<50 nm) that are heterogeneously distributed in the grains. The euhedral crystals at the exterior of the intergrowths have a lower porosity than the anhedral grains in the center of the intergrowths (Fig. 2c). We observe that the crystals associated with amorphous silicates (43.1 wt% SiO_2, 56.9 wt% FeO) mimic the texture of the amorphous materials, showing an increased porosity at the transition between these two phases (Fig. 2a). The fayalite crystals that have a high porosity also contain a high defect density compared to the low porosity crystals (Fig. 2c).

Discussion: Previous studies show that synthetic fayalite grows in the presence of aqueous fluids from disequilibrium reactions similar to the ones observed in chondrites [1-3]. These new microstructural observations indicate that the precipitation of fayalite crystals is controlled by two mechanisms. First, fayalite forms by direct crystallisation of the amorphous material in the presence of an aqueous fluid. In some regions, we observe that during this process, the texture, especially the porosity of the fayalite crystals, could be controlled by the texture of the amorphous materials, which probably has an effect on the fluid migration and possibly increases the element transport and reaction rates. Additionally, the porosity could be produced by (1) the fluid trapped and released from the amorphous material in the olivine, or by (2) a reduction in volume from the amorphous silicates, which is very low density to the denser fayalitic olivine. Second, fayalite crystals form by

direct precipitation from a supersaturated fluid via non-uniform lateral growth, which suggests that the crystal surface advances by lateral motion of steps, and not as the entire surface normal to itself. Previous studies show that crystals growing in highly supersaturated solutions have rougher, irregular surfaces (on a macroscopic rather than molecular scale) than those growing in low supersaturation solutions [4-5]. However, these surface irregularities have not been seen in chondrites. The presence of irregular surfaces and the high defect densities in the porous regions could indicate rapid crystallization (the duration of the experiment - 6 days) of fayalite crystals from a chemically-evolving aqueous fluid.

These fayalite crystals show multiple similarities to the olivines identified in other chondrites, such as Allende, and Krymka [6-8]. Therefore, they represent a tremendous opportunity to enhance our understanding of (1) the reactions between aqueous fluids with primordial solids and the formation of secondary phases and (2) the distribution and the concentration of fluids in the parent bodies of meteorites.

Acknowledgements: This work was funded by NASA grant NNH18ZDA001N-EW to ED..

References: [1] Dobrica E. et al. (2017) *Lunar and Planetary Sci.* 48, #2865. [2] Dobrica E. et al. (2017) *Annual Meeting of the Meteoritical Society* 80, #6342. 48, #2865. [3] Dobrica and Brearley (2021) *Meteoritics and Planetary Sci.* 13610 (in press). [4] Pantaraks P. et al., (2007) *Cryst. Growth Des.* 7, 2635–2642. [5] Galbraith S. C. et al., (2016) *Chem. Eng. Technol.* 39, 199–207. [6] Brearley, A. J. (1999) *Science* 285, 1380-1382. [7] Brearley A. J. (2009) *Lunar and Planetary Sci.* 40, #1791. [8] Weisberg M. K. et al. (1197) *Meteoritics and Planetary Sci.* 33, 1087-1099.

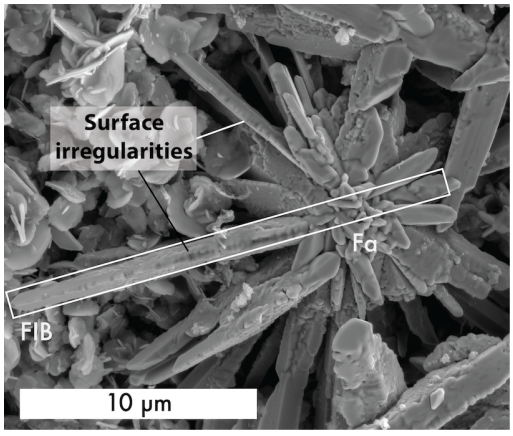

Figure 1. Secondary electron SEM micrograph of the hydrothermal experiment products showing radiating, intergrowths of fayalite (Fa) crystals with irregular surfaces. The white rectangle shows the regions where one of the focused ion beam sections (FIB, Fig. 1b-c) was prepared for TEM studies.

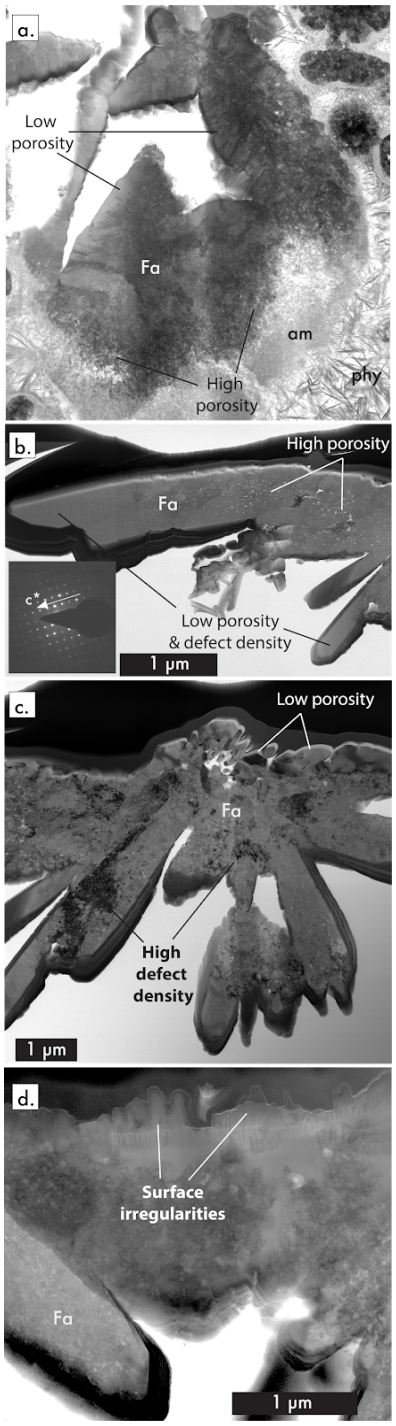

Figure 2. Bright-field STEM images showing the heterogeneous distribution of pores and defect density, the surface irregularities, and the minerals associated (am - amorphous silicates, phy - phyllosilicates) with the synthetic fayalite (Fa) crystals. The nanodiffraction pattern of the elongated euhedral olivine shows that the crystal is elongated parallel to the [001] direction (*c**).